

Advanced Boost Converter for Multi-Functional EV Charger

Laxmi Metagudd¹, Dr. S.G Srivani²

¹Student, EEE Department, RV Engineering College, Bangalore, Karnataka

²Associate Professor and PG Dean, EEE Department, RV Engineering College, Bangalore, Karnataka.

Submitted: 01-06-2021

Revised: 14-06-2021

Accepted: 16-06-2021

ABSTRACT: The EV is emerging as a promising solution to the problem caused by the fossil fuel powered vehicles. An integration of solar PV panel with EV not only useful for creating renewable energy based charging infrastructure but also compensate the negative impact of each other on the distribution grid. Effective photovoltaic power conditioning requires efficient power conversion. The main objective is to design the isolated boost converter (IBR) with accurate maximum power point tracking (MPPT) using P&O algorithm to counteract the effects of panel mismatch, shading, and general variance in power output during a daily cycle. The proposed isolated boost resonance (IBR) converter meets all requirements and gives high efficiency compared to the conventional converter. The IBR converter was designed for the solar PV input voltage ratings of 41.7V, input current 8.1A, 336W rated power and frequency 100 kHz. The converter circuit was simulated in PSIM software. The proposed converter boosts the output voltage of 360V was observed from simulation results.

KEYWORDS: Isolated Boost Resonant Converter (IBR), PSIM, P&O, MPPT.

I. INTRODUCTION

The main downside to electric vehicle (EV) technology is that energy from conventional sources is inadequate, so it cannot maintain the impact of EV demand. The renewable energy sources such as solar, wind is considered as alternative source to fossil fuel. The solar energy is abundant natural resource, which is freely available and is used as energy source to charge the EV battery.[1]

The main drawback of solar energy is that it is not available all the time due its intermittent nature. Therefore, charging EV battery with only solar energy may not be reliable. By integrating solar energy with grid support EV charging system. Whenever solar is not available to charge the battery, during that time grid supports in charging

the EV battery. Correspondingly, when solar PV is generating ample amount of power to charge EV, the excess amount of power is supplied back to the grid.[2]-[5]

Due to the varying climatic condition solar power obtained is not constant throughout the day and also the initial setup cost of the solar photovoltaic (SPV) is high, to overcome this situation MPPT (maximum power point tracking) is needed and maximum available power must be extracted from the SPV to offset the cost of the SPV. Therefore, an effective power converter is required to improve the power level for maintaining DC bus voltage requirements. [6]-[9]

The power converter for solar photovoltaic (PV) application requires an adaptive converter that is able to respond to the change in input current and voltage due to varying irradiation conditions. The solar PV array voltage varies continuously with operating temperature and panel construction and PV panel current varies with change in solar irradiance and shadow conditions.[10] The solar PV with MPPT is integrated with the EV charger with the bidirectional flow of power. The distributed generating MPPT gives better harvesting of energy compared to the centralized power generation. [11]. From the literature survey, solar PV units connected in parallel gives more efficiency in low light and partial shading conditions compared to series connected PV system.

The proposed isolated boost resonant converter (IBR) integrates the conventional boost converter into the DC-DC isolation transformer with a single inductor. The P&O algorithm is used for MPPT condition by sensing PV voltage and current. The proposed converter uses resonance condition (ZVS and ZCS) at the switches, thereby improves the efficiency of the converter by reducing switching losses. For PV application, the proposed converter satisfies the need for galvanic

isolation, easy gate drive control and low switching

loss.[12]-[17]

II. ADVANCED BOOST CONVERTER FOR MULTI-FUNCTIONAL EV CHARGER

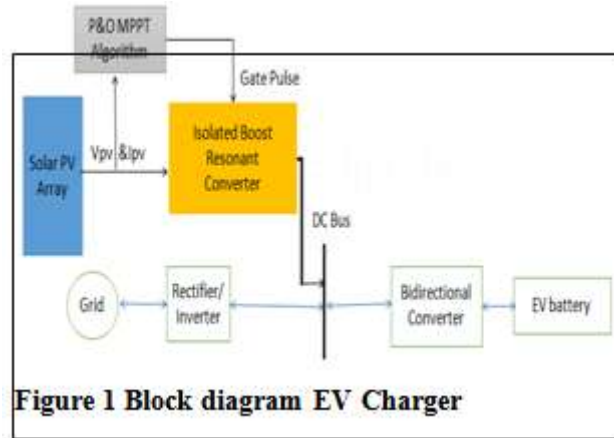


Figure 1 Block diagram EV Charger

The proposed multi-functional EV charger is shown in Figure 1. The charger operates with both SPV array and the grid and power not only flows for charging the vehicle battery as in a conventional charger but it also flows between all the three sources of energy. SPV array injects the generated electric energy into the DC link to charge the vehicle battery and to support the grid with excess energy.

The proposed IBR converter is shown in Figure 2, the input is connected to SPV array. The

MPPT P&O algorithm adjusts the duty ratio of IBR converter to achieve the MPPT condition by sensing the PV voltage and current. The soft switching operation (ZVS and ZCS) at Mosfet Q1 and diode D1 is used to reduce the switching losses, by this converter efficiency improves. Secondary side doubler circuit is used to double the voltage from 200V to 400V.

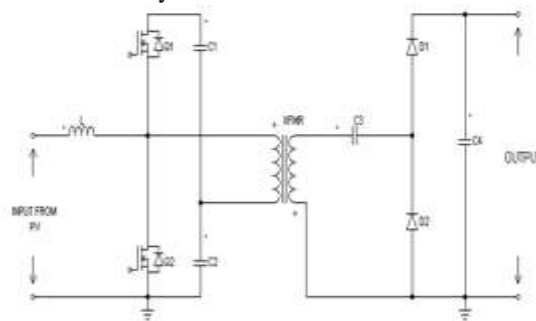


Figure 2 Advanced Boost Converter.

The high frequency transformer is used to increase the voltage level and also to isolate PV system from faults occurring at the grid. The secondary side voltage doubler circuit is used to reduce the size of the transformer and ratings of the components.

Mode-1 Operation: When MOSFET Q1 is On and MOSFET Q2 is OFF, the voltage across each capacitor, which are in series, is V_{in} each. And the

total voltage across both the capacitors is $2V_{in}$. Therefore, the voltage appearing across the primary of the transformer is V_{in} . With the transformer being inverted, and for a turns ratio of $n = \frac{V_s}{V_p}$, (V_s is secondary voltage and V_p is Transformer primary voltage), $V_s = -(n \cdot V_p)$. This forward biases D2 and reverse biases D1. Thus C3 charges to V_s through D2.

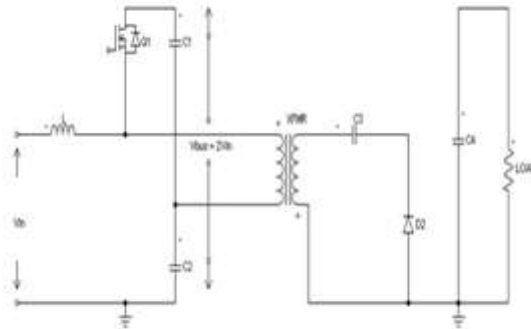


Figure 3 Mode-1 Operation when Mosfet Q1 is On

Mode-2 Operation: When Q1 is turned OFF and Q2 is turned on at the next half cycle, the input current goes through Q2 and at the same time, with C2 alone in the picture, C2 resonates with the LK, and the transformer current also goes through MOSFET (Path is C2 – XFMR – Q2). Thus current in Q2, $I_{Q2} = \text{Transformer current} + \text{input current}$. Now, the primary voltage ($V_p = 2V_{in}$) is reflected at the secondary side, and the secondary voltage is

$V_s = n \cdot V_p$. With C3 previously charged with V_s and with additional V_s , the net potential is $2V_s$ causing D1 to forward bias, charging C4 with $2V_s$. Note that the combination C3, C4, D1 and D2 is a voltage doubler. So, whatever voltage comes at the secondary, it is again doubled at C4. And here, at the end of the second half of the cycle, voltage at C4 is $2V_s$, as expected.

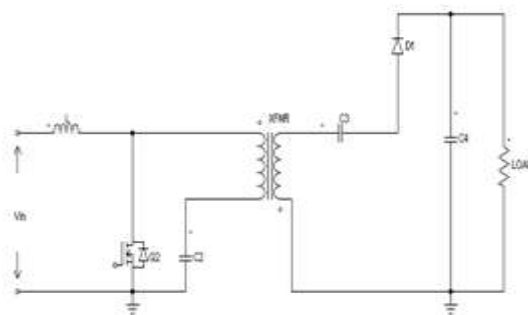


Figure 4 Mode-2 Operation when Mosfet Q2 is ON

The figure 5 represents the waveforms during two modes of the operation. The current through the switch I_{Q1} , I_{Q2} , resonant capacitor C1, C2 and C3 and diode current D1 and D2 during switching operation is shown.

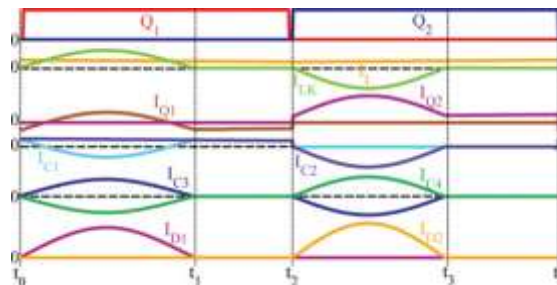


Figure 5 timing diagram showing circuit operation

III. DESIGN OF THE IBR CONVERTER

1. Duty ratio for input requirements: By setting the maximum and minimum duty ratio the V_{min} and V_{max} range is obtained from equation (1)

$$D_{max} = \frac{V_{in,max}}{V_{in,min} + V_{in,max}} \quad (1)$$

$$D_{min} = 1 - D_{max} \quad (2)$$

The 50% duty ratio is obtained at nominal input voltage, the dc bus voltage V_{bus} is obtained across the resonance capacitor $C1$ & $C2$.

$$V_{bus} = V_{in, min} + V_{in, max} \quad (3)$$

2. Input Inductor Design: In PV application the inductor L is calculated based on maximum ripple current ΔI_L .

$$L = \frac{V_{bus} * T_{sw}}{4 * I_{Lavg} * \% \Delta I_{Lmax}} \quad (4)$$

3. Transformer Design: The transformer turns ratio (n) is calculated based V_{bus} voltage and desired output voltage V_{out} ,

$$n = \frac{N_{sec}}{N_{pri}} = \frac{V_{out}}{V_{bus}} \quad (5)$$

4. Maximum resonant period lengths: The maximum & minimum duty ratios are known from equation-1 & 2. By assuming desired switching frequency, resonant period T_{res1} & T_{res2} are obtained.

$$T_{res1, max} = (1 - D_{max}) * T_{sw} \quad (6)$$

$$T_{res2, max} = D_{min} * T_{sw} \quad (7)$$

5. Resonant Capacitor $C1$ and $C2$: Based resonant time period calculated from equation (6) & (7) obtain the value of $C1$ & $C2$ assuming $C3$ capacitor, L_k is transformer leakage inductance,

$$T_{res1} = \pi \sqrt{L_k \left(\frac{n^2(C1+C2)(C3)}{C1+C2+n^2*C3} \right)} \quad (8)$$

$$T_{res2} = \pi \sqrt{L_k \left(\frac{n^2*C2*C3}{C2+n^2*C3} \right)} \quad (9)$$

IV. SIMULATION AND RESULTS

The selected topology is simulated in PSIM Software. The ZVS and ZCS resonance condition is observed and performance of the

converter is checked. Table 1 shows the parameters values considered for the PSIM simulation of the circuit.

Table: 1 Parameters of Simulation

Parameters	Ratings
Open circuit Voltage V_{oc}	53V
Short Circuit Current I_{sc}	8.1A
Irradiance	1000W/m ²
Temperature	100 °C
Input inductor L	8mH
Resonance Capacitor C1, C2, and C3	10uF, 10uF and 0.1uF
Switching Frequency	100 kHz
Load Resistance	
Transformer turns ratio	N1: N2 = 4:21

The simulation circuit for IBR is as shown in Figure 6. The IBR is supplied by PV physical module as shown in simulation circuit. The irradiance and temperature value for PV panel is set as 1000W/m² and 25°C using constant block.

Solar PV panel open circuit voltage, short circuit current, MPPT Voltage and MPPT Power is set as per the simulation parameter Table 1. The secondary side doubler circuit is used to increase

the transformer secondary voltage from 200V to 400V.

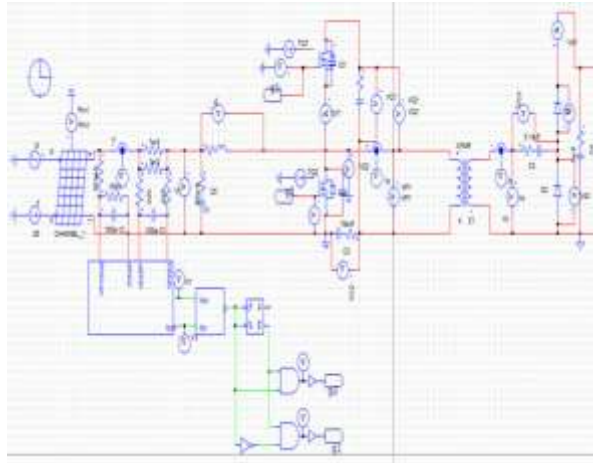


Figure 6 Simulation Circuit Advanced Boost Converter

The MPPT sub-block is shown in figure 7. The P&O algorithm is used to achieve MPPT condition. The PWM pulses for mosfets are generated based on change in duty ratio. According P&O method change in PV voltage and change in PV power is obtained using differential block and

the change in (dv) & (dp) is compared with respect to ground and given to exor gate. The error value is given to PI Controller block with $K_p=1$ and $K_i=0.01$. The signal from controller is compared with ramp signal. The complimentary generated pulses are given to MOSFET Q1 and Q2.

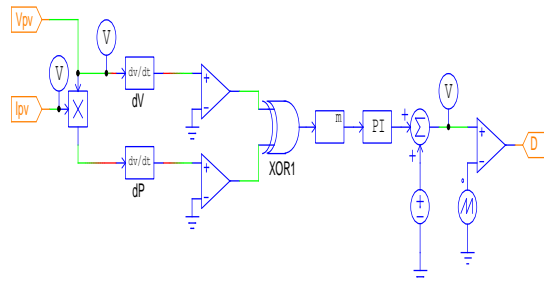


Figure 7 MPPT Sub-block

The Figure 8 shows the transformer primary and secondary current waveforms. The CLC resonance condition is observed in below figure. The transformer primary and secondary current observed is $I_p=10.39A$ and $I_s=2.09A$

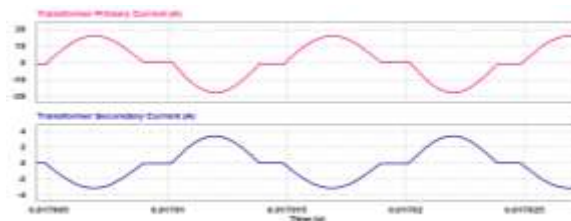


Figure 8 Transformer primary & secondary current waveforms

The MOSFET Q1 voltage and current waveform are shown in figure 9. The Voltage across the switch is observed as twice the input PV voltage. The RMS voltage and current of the MOSFET Q1 is $V_{q1}=53.2V$ and $I_{q1}=3.94A$ and MOSFET Q2 is $V_{q2}=45.49V$ and $I_{q2}=14.12A$.

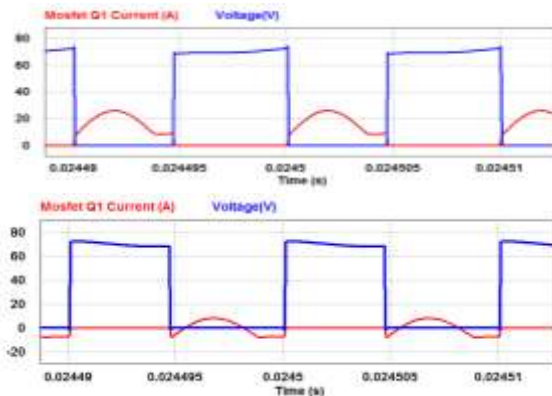


Figure 9 MOSFET Q1 & Q2 Voltage & Current Waveforms.

Resonance capacitor C1 and C2 current waveforms are shown in figure 10. The capacitor C1 is resonate when MOSFET Q1 is ON and

capacitor C2 resonate when MOSFET Q2 is ON. The average current flowing through capacitor C1 and C2 is $I_{c1}=0.95A$, $I_{c2}=1.94A$.

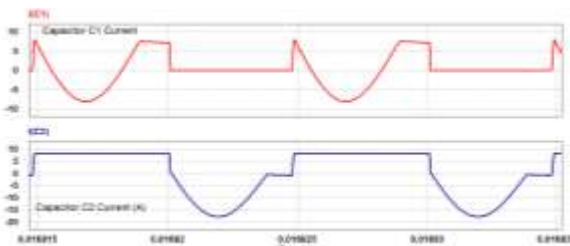


Figure 10 Resonance capacitor C1 & C2 current waveforms

The output Voltage and current waveforms of IBR circuit is shown in Figure 11. The average output voltage and current is $V_o=360.29V$, $I_o=0.816A$.

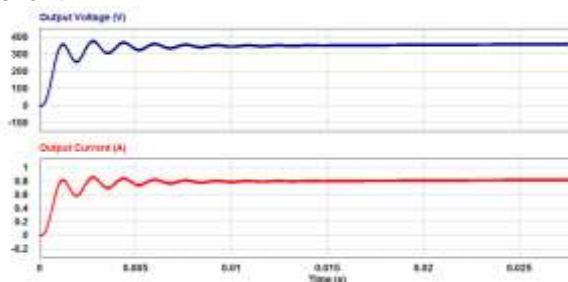


Figure 11 Output Voltage & current waveforms

V. CONCLUSION

The purpose of multi-functional EV charger with integration of solar PV array and grid to charge EV battery, which is connected to DC Bus, is presented in this work. An isolated boost resonant converter is proposed as a solution to provide efficient, distributed PV power conversion. The circuit topology is a hybrid between a series resonant half bridge and traditional CCM boost converter, which uses only two active switches. The IBR converter topology was described with the circuit operating modes and waveforms. The proposed converter gives better efficiency

compared to conventional converter with less component and easy control technique using P&O algorithm.

REFERENCES

- [1]. Anjeet Verma, Bhim Singh ,Ambrish Chandra & Kamal Al-Haddad, “ An Implementation of Solar PV Array Base Multifunctional EV Charger”, IEEE journal ,vol. 3, no. 3, pp. 81-88,2020.
- [2]. Anjeet Verma, Bhim Singh, “Multi-Functional Charger for Electric Vehicle Operating with Grid and SPV Generation”,

- IEEE transactions, vol. 6, no. 4, pp 1-1484, 2017.
- [3]. Anjeet Verma, Bhim Singh, "Multi-objective Reconfigurable Three Phase Off Board Charger for EV", IEEE Transportation Electrification Conference, vol-10, no-3, pp1917-1926, 2017.
- [4]. M. Premchand and S. K. Gudey, "Solar based Electric Vehicle Charging Circuit in G2V and V2G modes of Operation," 2020 IEEE Students Conference on Engineering & Systems (SCES), pp. 1-6, 2020.
- [5]. O. M. Abdelwahab and M. F. Shaaban, "PV and EV charger allocation with V2G capabilities," 2019 IEEE 13th International Conference on Compatibility, Power Electronics and Power Engineering (CPE-POWERENG), pp. 1-5, 2019.
- [6]. D. Jung, Y. Ji, S. Park, Y. Jung and C. Won, "Interleaved Soft-Switching Boost Converter for Photovoltaic Power-Generation System," in IEEE Transactions on Power Electronics, vol. 26, no. 4, pp. 1137-1145, April 2011.
- [7]. B. York, W. Yu and J. Lai, "An Integrated Boost Resonant Converter for Photovoltaic Applications," in IEEE Journal Transactions on Power Electronics, vol. 28, no. 3, pp. 1199-1207, March 2013.
- [8]. P. H. Kydd, J. R. Anstrom, P. D. Heitmann, K. J. Komara and M. E. Crouse, "Vehicle-SolarGrid Integration: Concept and Construction," IEEE Power and Energy Technol. Sys. J, vol-3, no-3, pp.81-88, Sept. 2016.
- [9]. D. Jung, Y. Ji, S. Park, Y. Jung and C. Won, "Interleaved Soft-Switching Boost Converter for Photovoltaic Power-Generation System," in IEEE Transactions on Power Electronics, vol. 26, no. 4, pp. 1137-1145, April 2011.
- [10]. Y. Wang et al., "Storage-Less and Converter-Less Photovoltaic Energy Harvesting With Maximum Power Point Tracking for Internet of Things," IEEE Transactions on Computer-Aided Design of Integrated Circuits and Systems, vol. 35, no. 2, pp. 173-186, Feb. 2016.
- [11]. M. A. G. de Brito, L. Galotto, L. P. Sampaio, G. d. A. e Melo and C. A. Canesin, "Evaluation of the Main MPPT Techniques for Photovoltaic Applications," IEEE Journal Transactions on Industrial Electronics, vol. 60, no. 3, pp. 1156-1167, March 2013.
- [12]. S. K. Kollimalla and M. K. Mishra, "Variable Perturbation Size Adaptive P&O MPPT Algorithm for Sudden Changes in Irradiance," IEEE Transactions on Sustainable Energy, vol. 5, no. 3, pp. 718-728, July 2014.
- [13]. Wang, W. Liu, H. Ma and L. Chen, "Resonance Analysis and Soft-Switching Design of Isolated Boost Converter With Coupled Inductors for Vehicle Inverter Application," IEEE Journal Transactions on Power Electronics, vol. 30, no. 3, pp. 1383-1392, March 2015.
- [14]. Daneil W, "Power Electronics", McGraw-Hill Education, 16 Feb 2010.
- [15]. "Soft-Switching PWM Full-Bridge Converters: Topologies, Control, and Design", publication 2014.
- [16]. A.V.J.S. Praneeth, Najath A Azeez, Lalit Patnaik, Sheldon S Williamson, "Proportional Resonant Controllers in On-board Battery Chargers for Electric Transportation", IEEE International Conference on Industrial Electronics for Sustainable Energy Systems (IESES), pp.237-242, 2018.
- [17]. Bhim Singh, Anjeet Verma, A. Chandra and Kamal Al-Haddad "Implementation of Solar PV-Battery and Diesel Generator Based Electric Vehicle in IEEE International Conference on Power Electronics, Drives and Energy Systems (PEDES), 2018.